

# Pd AND Re ISOTOPE PRODUCTION IN THE FIELD OF MIXED X,n-RADIATION OF ELECTRON ACCELERATOR

*N.P. Dikiy, V.A. Kushnir, Yu.V. Lyashko, V.V. Mitrochenko, S.A. Perezhogin, Yu.V. Rogov, A.Eh. Tenishev, A.V. Torgovkin, V.L. Uvarov, V.A. Shevchenko, I.N. Shlyakhov,*

*B.I. Shramenko*

*National Science Center "Kharkov Institute of Physics and Technology", Kharkov, Ukraine*

*E-mail: uvarov@kipt.kharkov.ua*

Radioactive isotopes of palladium ( $^{103}\text{Pd}$ ) and rhenium ( $^{186}\text{Re}$  and  $^{188}\text{Re}$ ) have found wide use in nuclear medicine. The present report deals with the conditions for their production by a photonuclear method at an electron accelerator. Studies have been made into the channels of target isotope/attendant impurity production as palladium and rhenium targets of natural isotopic composition were exposed to a mixed flux of X-ray (bremsstrahlung) with endpoint energy of 40 MeV and photoneutrons. By placing a bremsstrahlung converter and the target inside a neutron moderator, data have been obtained for the effect of photoneutron spectrum on the isotope yield. The simulation technique has been used to investigate the photonuclear yield of target isotopes and major impurities as function of electron energy.

PACS: 07.85.-m, 81.40wx,87.53-j,87.53Wz

## INTRODUCTION

Radioactive sources based on the isotopes  $^{103}\text{Pd}$  ( $E_x \sim 20$  keV;  $T_{1/2} = 16.9$  days),  $^{186}\text{Re}$  ( $E_\beta = 346.7$  keV;  $E_\gamma = 137.2$  keV;  $T_{1/2} = 89.2$  hours) and  $^{188}\text{Re}$  ( $E_\beta = 764.3$  keV;  $E_\gamma = 155.0$  keV;  $T_{1/2} = 17$  hours) are used in current medicine for brachytherapy.

Until recently, a common practice for  $^{103}\text{Pd}$  production has been to use the reactor technique, which consisted in neutron irradiation of palladium targets enriched in the  $^{102}\text{Pd}$  isotope [1], and also, to employ a cyclotron technology for carrier-free production of the target isotope [2]. The market demand for  $^{103}\text{Pd}$  is so great that in the USA only, its production is provided by more than 10 cyclotrons.

As regards  $^{186}\text{Re}$  isotope sources, they are produced at reactors through thermal neutron irradiation of either rhenium powder enriched in the  $^{185}\text{Re}$  isotope [1] or a natural rhenium wire [3]. Attempts of carrier-free production of the  $^{186}\text{Re}$  isotope with the use of a cyclotron have also been made [4].  $^{188}\text{Re}$  is generally obtained as a result of decay of the generating  $^{188}\text{W}$  isotope, which is produced in high-flux reactors through the double neutron capture by the tungsten target enriched in the  $^{186}\text{W}$  isotope [1].

In view of the tendency to gradually abandon the reactor technologies [5], and also, considering a high cost of cyclotron-produced isotopes, it appears of interest to investigate the conditions of isotope production at relatively inexpensive and ecologically safe electron accelerators.

## 1. PRINCIPAL REACTIONS

Natural palladium presents a mixture of 6 stable isotopes:  $^{102}\text{Pd}$  (1.02%),  $^{104}\text{Pd}$  (11.14%),  $^{105}\text{Pd}$  (22.33%),  $^{106}\text{Pd}$  (27.23%),  $^{108}\text{Pd}$  (26.46%) and  $^{110}\text{Pd}$  (11.72%).  $^{103}\text{Pd}$  can be generated in the field of bremsstrahlung radiation at an electron accelerator due to the reaction  $^{104}\text{Pd}(\gamma, n)^{103}\text{Pd}$ . To provide a sufficient flux of bremsstrahlung photons in the giant resonance region, the electron energy must range between 35 and 40 MeV. In this case, there arises one more photonuclear channel of desired isotope generation, viz.,  $^{105}\text{Pd}(\gamma, 2n)^{103}\text{Pd}$ . Besides, the process of electron radiation conversion into

bremsstrahlung is accompanied by generation of photoneutrons (e.g., see Ref. [6]). These may give rise to the  $^{102}\text{Pd}(n, \gamma)^{103}\text{Pd}$  reaction, too.

Natural rhenium consists of two isotopes:  $^{185}\text{Re}$  (37.4 %) and  $^{187}\text{Re}$  (62.6%). To generate  $^{186}\text{Re}$  at an electron accelerator, the reactions  $^{187}\text{Re}(\gamma, n)^{186}\text{Re}$  and  $^{185}\text{Re}(n, \gamma)^{186}\text{Re}$  can be used. Under the action of photoneutrons, natural rhenium can also yield  $^{188}\text{Re}$  through the  $^{187}\text{Re}(n, \gamma)^{188}\text{Re}$  reaction.

It is known that the neutron radiative-capture cross-sections in the thermal region increase by one order of value or more. Therefore, for simultaneous engaging the photonuclear and neutron-capture channels, it has been suggested that the bremsstrahlung converter and the isotopic target should be placed inside the neutron moderator [7].

## 2. EXPERIMENT

2.1. For measuring the isotope yields during exposure of targets to a mixed X,n-radiation with and without the neutron moderator, an output device has been developed, the schematic of which is presented in Fig. 1. The device includes an aluminum tube 1, which is axially symmetric to the electron beam axis of the accelerator A and accommodates the bremsstrahlung converter C and the target T. The converter consists of four tantalum plates, each 1 mm thick and 30 mm in diameter, separated by same-size air gaps to provide cooling. The target includes the enclosed in aluminum holder 3 aluminum locking discs 4 and 8, each 20 mm in diameter and 3 mm thick. The discs are separated by a 0.1 mm thick molybdenum foil-monitor 5, and a 3 mm thick aluminum spacer having a cell of diameter 10 mm, where the isotopic targets 7 were located.

All the targets, except rhenium, presented foil fragments of maximum size no more than 5 mm. The rhenium powder was placed in an aluminum thin-walled capsule with an inside diameter 8 mm, and 4 mm in height.

2.2. The fluence of bremsstrahlung photons on the isotopic targets was controlled against the yield of the reference reactions in the foil-monitor 5. Natural molybdenum comprises seven stable isotopes, including  $^{92}\text{Mo}$  (14.84%),  $^{98}\text{Mo}$  (24.13%) and  $^{100}\text{Mo}$  (9.63%). The photon fluence can be estimated against the  $^{90}\text{Mo}$

( $T_{1/2}=5.7$  hours) yield by the  $^{92}\text{Mo}(\gamma, 2n)^{90}\text{Mo}$  reaction, because  $^{90}\text{Mo}$  can be generated only in this channel. In turn, the isotope  $^{99}\text{Mo}$  ( $T_{1/2}=66.02$  hours) can be generated in the two reactions at once:  $^{100}\text{Mo}(\gamma, n)^{99}\text{Mo}$  and  $^{98}\text{Mo}(n, \gamma)^{99}\text{Mo}$ . So the comparison between the  $^{90}\text{Mo}$  and  $^{99}\text{Mo}$  yields, normalized to the electron beam charge on the converter, enables one to estimate the contribution of each of the channels. To determine the profile of the high-energy photon flux, at the converter output a 0.1 mm thick tin-foil 9, measuring 40×40 mm, was placed, which was activated together with the isotope target. The profile of the photon flux was reconstructed by measuring the 2D-distribution of the foil 9 surface activity using a gamma-scanner [8].

2.3. To measure the isotope yield as a result of a combined action of the bremsstrahlung and moderated photoneutrons, the system with the converter and the target was arranged inside the moderator M. The detailed description of the latter can be found in Ref. [7]. In this case, at point 10 of the output device one more isotopic target was placed so that the distance from the target to the beam axis corresponded to the distance from the target 7 to the converter. Each target comprised samples of palladium, rhenium and gold. The latter were used as activation detectors. In this way, the target 7 experienced the action of a mixed flux of bremsstrahlung and soft photoneutrons, whereas the target 10 was exposed mostly to neutrons.

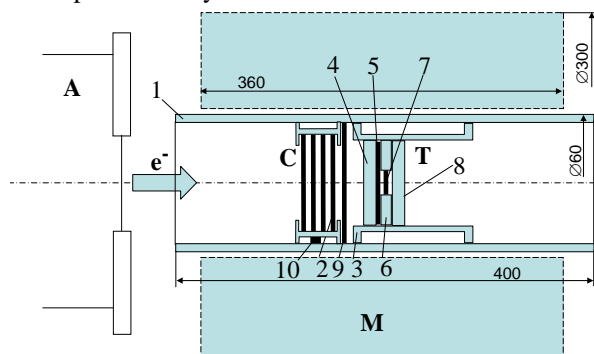


Fig. 1. Schematic of output device

2.4. The targets were irradiated at the NSC KIPT accelerator LU-40 [9] for 2 hours at an electron energy of 40 MeV, the beam pulse length of 1.5  $\mu\text{s}$ , the pulse repetition frequency 50 Hz, and the average current 4.1  $\mu\text{A}$ . The electron beam profile on the converter corresponded to the Gaussian distribution with the FWHM 1.2 cm. The FWHM of the beam energy spectrum was no more than 2%. Fig. 2 shows the measured profile of the X-Ray flux.

After each exposure, the targets were cooled for 24 hours to provide the decay of induced activity caused by short-lived impurities.

The isotope activity in the samples was determined with the use of the gamma-spectrometer based on the Canberra HPGc detector with the analyzer InSpector-2000 and the software Genie 2000. The detector provides the relative registration efficiency of 20 % and the energy resolution of 1.8 keV at a photon energy of 1332 keV (Co-60). The error of specific isotope activity measurement varied within the 7...10% range. The data obtained were normalized to the electron-beam charge value in the course of the target activation.

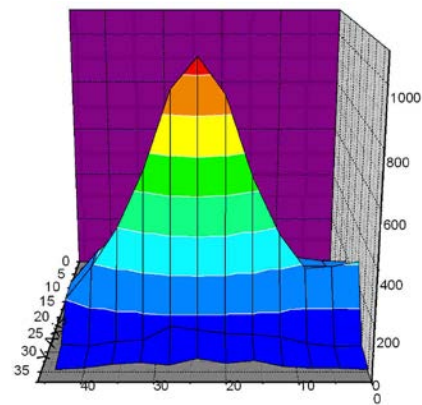


Fig. 2. X-Ray flux distribution behind the converter

2.5. An independent analysis of the target photoactivation processes was performed by a simulation method based on the modified transport code PENELOPE-2008 [10]. The yield of photonuclear reactions was calculated by summing their microyields along all the trajectories of all above-threshold photons in the corresponding target device elements [11]. The reaction cross-sections were taken from the database [12]. The processes of target activation by neutrons were not simulated.

### 3. RESULTS AND DISCUSSION

Tables 1 and 2 present the data on the principal isotope yield obtained experimentally and by the simulation method (in brackets the mass of each target in mg is given). Their analysis shows that the calculated photonuclear yield of  $^{101}\text{Pd}$ ,  $^{184}\text{Re}$  in the isotopic targets, and also, of  $^{90}\text{Mo}$  and  $^{196}\text{Au}$  in the targets-monitors (Table 3) located on the electron beam axis, are in satisfactory agreement with the experimental results. This bears witness to a sufficiently exact description of the reaction cross sections, as well as to adequacy of their computer simulation. The last fact gives grounds for calculation of isotope yields at different modes of target activation. Thus, Figs. 3 to 6 show the yields of  $^{103}\text{Pd}$  and  $^{186}\text{Re}$ , and also, of the major impurities as function of the electron energy and activation time expressed in terms of half-life of the desired isotope.

The yield of  $^{188}\text{Re}$  from the Re target 7 without the moderator was determined to be 0.2  $\mu\text{Ci}/\text{hour}\cdot\mu\text{A}\cdot\text{g}$ . In the presence of the moderator, the yields of  $^{188}\text{Re}$  and  $^{198}\text{Au}$  in the samples situated on the beam axis and sideways were found to be nearly the same. This confirms the closeness between the values of neutron fluxes acting on the targets, and permits one to estimate the contribution of neutron-capture channels to the yields of desired isotopes.

In the case of palladium, the  $^{102}\text{Pd}(n, \gamma)$  reaction provides no more than 1.5 % of the total yield of  $^{103}\text{Pd}$ , this being within the total measurement error. It should be noted that the photonuclear yield of  $^{103}\text{Pd}$  was calculated with account of the  $^{104}\text{Pd}(\gamma, n)^{103}\text{Pd}$  reaction only. So the experimentally observed excess can be explained by the contribution of the  $^{105}\text{Pd}(\gamma, 2n)^{103}\text{Pd}$  channel. In its turn, the  $^{185}\text{Re}(n, \gamma)$  reaction adds ~10 % to the total yield of  $^{186}\text{Re}$ . Note that with the use of the moderator, the production of  $^{188}\text{Re}$  increases by more than ten times.

Table 1

Isotope yields in Pd targets

| Isotope           | T <sub>1/2</sub> , days | Reaction                                   | Yield, μCi/hour·μA·g |                      |                    |
|-------------------|-------------------------|--|----------------------|----------------------|--------------------|
|                   |                         |  | Pd-7 (83.5)          |                      | Pd-10 (84.3)       |
|                   |                         |  | Simulated            | Experimental         | Experimental       |
| <sup>103</sup> Pd | 16.9                    | <sup>104</sup> Pd(γ, n) <sup>103</sup> Pd  | 1.8                  | 3.3                  | 0.05               |
|                   |                         | <sup>105</sup> Pd(γ, 2n) <sup>103</sup> Pd | -                    |                      |                    |
|                   |                         | <sup>102</sup> Pd(n, γ) <sup>103</sup> Pd  | -                    |                      |                    |
| <sup>100</sup> Pd | 3.63                    | <sup>102</sup> Pd(γ, 2n) <sup>100</sup> Pd | -                    | 8.6·10 <sup>-2</sup> | 8·10 <sup>-4</sup> |
| <sup>101</sup> Pd | 0.34                    | <sup>102</sup> Pd(γ, n) <sup>101</sup> Pd  | 7.6                  | 7.0                  | 0.073              |
| <sup>109</sup> Pd | 0.56                    | <sup>110</sup> Pd(γ, n) <sup>109</sup> Pd  | -                    | 62.5                 | 1.6                |
|                   |                         | <sup>108</sup> Pd(n, γ) <sup>109</sup> Pd  | -                    |                      |                    |
|                   |                         | <sup>110</sup> Pd(γ, p) <sup>109</sup> Rh→ | -                    |                      |                    |
| <sup>105</sup> Rh | 1.47                    | <sup>106</sup> Pd(γ, p) <sup>105</sup> Rh  | -                    | 2.0                  | 0.02               |
|                   |                         | <sup>105</sup> Pd(n, p) <sup>105</sup> Rh  | -                    |                      |                    |
|                   |                         | <sup>108</sup> Pd(n, α) <sup>105</sup> Ru→ | -                    |                      |                    |

Table 2

Isotope yields in Re targets

| Isotope           | T <sub>1/2</sub> , days | Reaction                                  | Yield, μCi/hour·μA·g |              |              |
|-------------------|-------------------------|---|----------------------|--------------|--------------|
|                   |                         |   | Re-7 (852)           |              | Re-10 (960)  |
|                   |                         |   | Simulated            | Experimental | Experimental |
| <sup>186</sup> Re | 3.72                    | <sup>187</sup> Re(γ, n) <sup>186</sup> Re | 49.8                 | 56.9         | 4.6          |
|                   |                         | <sup>185</sup> Re(n, γ) <sup>186</sup> Re | -                    |              |              |
| <sup>188</sup> Re | 0.71                    | <sup>187</sup> Re(n, γ) <sup>188</sup> Re | -                    | 3.30         | 3.25         |
| <sup>184</sup> Re | 38.0                    | <sup>185</sup> Re(γ, n) <sup>184</sup> Re | 2.9                  | 2.85         | 0.6          |

Table 3

Isotope yields in targets-monitors

| Target      | Isotope           | T <sub>1/2</sub> , days | Reaction                                  | Yield, μCi/hour·μA·g |              |
|-------------|-------------------|-------------------------|---|----------------------|--------------|
|             |                   |                         |   | Simulated            | Experimental |
| Mo-5 (312)  | <sup>99</sup> Mo  | 2.75                    | <sup>100</sup> Mo(γ, n) <sup>99</sup> Mo  | 4.69                 | 5.48         |
|             |                   |                         | <sup>98</sup> Mo(n, γ) <sup>99</sup> Mo   | -                    |              |
| Au-7 (111)  | <sup>196</sup> Au | 6.2                     | <sup>197</sup> Au(γ, n) <sup>196</sup> Au | 5.95                 | 5.15         |
|             | <sup>198</sup> Au | 2.7                     | <sup>197</sup> Au(n, γ) <sup>198</sup> Au | -                    | 2.65         |
| Au-10 (112) | <sup>196</sup> Au | 6.2                     | <sup>197</sup> Au(γ, n) <sup>196</sup> Au | -                    | 0.62         |
|             | <sup>198</sup> Au | 2.7                     | <sup>197</sup> Au(n, γ) <sup>198</sup> Au | -                    | 2.59         |

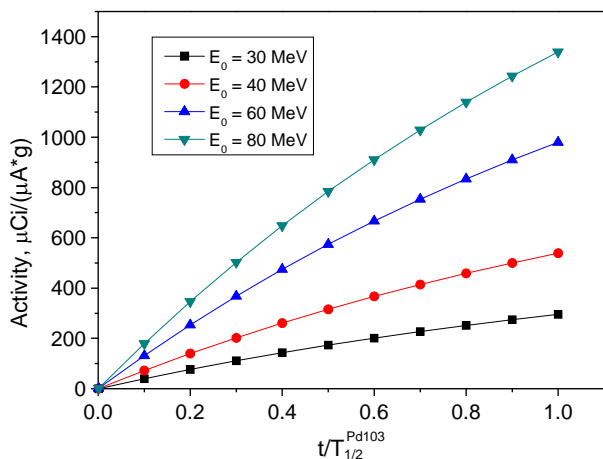


Fig. 3. Specific activity of <sup>103</sup>Pd versus time of exposure at different electron energies

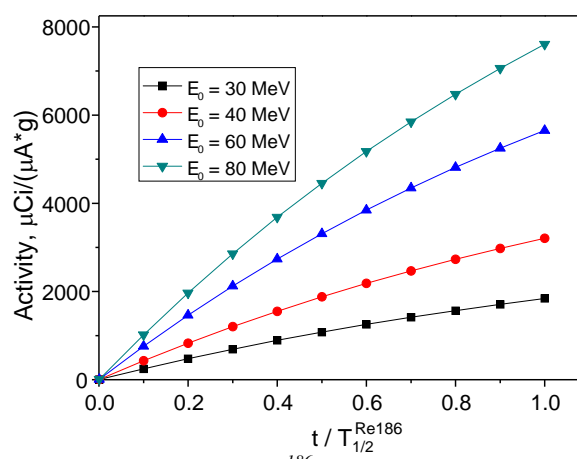


Fig. 4. Specific activity of <sup>186</sup>Re versus time of exposure at different electron energies

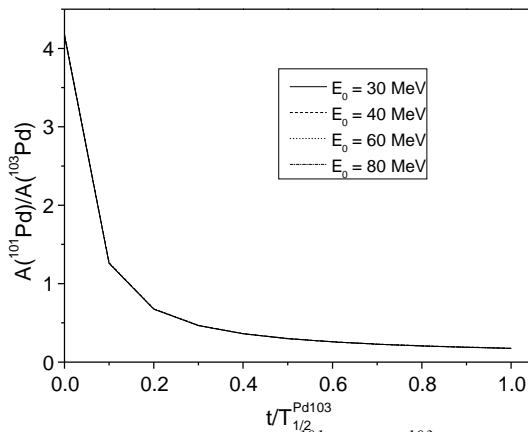


Fig. 5. Specific activities of  $^{101}\text{Pd}$  and  $^{103}\text{Pd}$  versus time of exposure

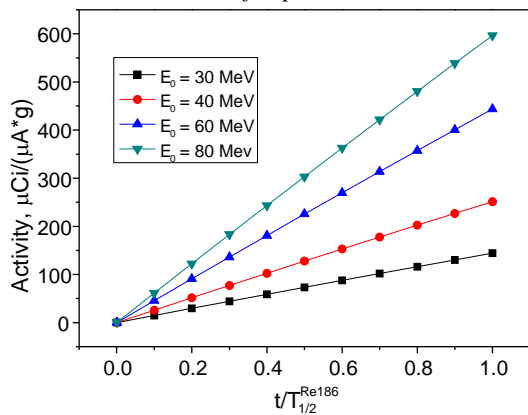


Fig. 6. Specific activity of  $^{184}\text{Re}$  versus time of exposure at different electron energies

## CONCLUSIONS

A satisfactory fit of experimental results and the simulation data on the photonuclear isotope yield makes it possible to calculate the yields in the thick technological targets and to compare different methods of isotope production (Tables 4 and 5). For example, from Table 4 it can be concluded that the cyclotron technology has a preference as to the specific and total yields of  $^{103}\text{Pd}$  alongside with a low level of impurities. At the same time, it involves a considerable amount of radiochemical procedures, and the produced isotope sources are beyond regeneration. The photonuclear method is capable of providing a high yield of  $^{103}\text{Pd}$  in case of using the targets enriched in the  $^{104}\text{Pd}$  isotope at much less expenses for the accelerator. In this case, the decayed sources can be reactivated an unlimited number of times.

As regards  $^{186}\text{Re}$  (see Table 5), an electron accelerator having routine parameters (40 MeV, 250  $\mu\text{A}$ ) can provide a considerably higher yield than the reactor and cyclotron technologies do. An additional gain in the yield, along with a reduction in the  $^{184}\text{Re}$  yield, can be provided by using the target enriched in  $^{187}\text{Re}$ . The cooled sources can also be reactivated. At the same time, the reactor method retains its advantage as to the specific yield of  $^{186}\text{Re}$ .

Table 4

Comparison between the methods of  $^{103}\text{Pd}$  production

| Facility, parameters   | Target, reaction, cross-section   | Yield  |  | Major impurities   |
|--|---|--|--|--|
|  |   | specific   | total  |  |
| Reactor [1]<br>$4 \cdot 10^{13} \text{ n/cm}^2 \cdot \text{s}$ | $^{102}\text{Pd}$ , $^{102}\text{Pd}(n, \gamma)$ , 3b   | 150 $\mu\text{Ci}/\text{hour} \cdot \text{g}$                        | 15 $\mu\text{Ci}/\text{hour}$                    | $^{109}\text{Pd}$ , $^{111}\text{Au}$  |
| Cyclotron [2]<br>20 MeV  | $^{\text{nat}}\text{Rh}$ , $^{103}\text{Rh}(p, n)$ , 505 mb<br>( $E_p=10 \text{ MeV}$ )           | $\sim 270 \mu\text{Ci}/\mu\text{A} \cdot \text{hour} \cdot \text{g}$ | 270 $\mu\text{Ci}/\mu\text{A} \cdot \text{hour}$ | Carrier-free   |
| Electron accelerator [13]<br>40 MeV                            | $^{\text{nat}}\text{Pd}$ , $^{104}\text{Pd}(\gamma, n)$ , 180 mb<br>( $E_\gamma=15 \text{ MeV}$ ) | 4 $\mu\text{Ci}/\mu\text{A} \cdot \text{hour} \cdot \text{g}$        | 50 $\mu\text{Ci}/\mu\text{A} \cdot \text{hour}$  | $^{100}\text{Pd}$ , $^{101}\text{Pd}$ ,<br>$^{109}\text{Pd}$ , $^{105}\text{Rh}$ |

Table 5

Comparison between the methods of  $^{186}\text{Re}$  production

| Facility, parameters   | Target, reaction, cross-section   | Yield   |   | Major impurities                      |
|--|---|---|---|---------------------------------------|
|  |   | specific  | total   |                                       |
| Reactor [1]<br>$3 \cdot 10^{14} \text{ n/cm}^2 \cdot \text{s}$ | $^{185}\text{Re}(>94\%)$ ,<br>$^{185}\text{Re}(n, \gamma)$ , 112b                                 | 7.5 $\text{Ci}/\text{hour} \cdot \text{g}$                          | 75 $\mu\text{Ci}/\text{hour}$                       | $^{188}\text{Re}$                     |
| Cyclotron [4]<br>14 MeV  | $^{\text{nat}}\text{W}$ , $^{186}\text{W}(p, n)$ , 80 mb<br>( $E_p=9 \text{ MeV}$ )               | $\sim 20 \mu\text{Ci}/\mu\text{A} \cdot \text{hour} \cdot \text{g}$ | 20 $\mu\text{Ci}/\mu\text{A} \cdot \text{hour}$     | Carrier-free                          |
| Electron accelerator [13]<br>40 MeV                            | $^{\text{nat}}\text{Re}$ , $^{187}\text{Re}(\gamma, n)$ , 420 mb<br>( $E_\gamma=14 \text{ MeV}$ ) | $\sim 60 \mu\text{Ci}/\mu\text{A} \cdot \text{hour} \cdot \text{g}$ | $\sim 1 \mu\text{Ci}/\mu\text{A} \cdot \text{hour}$ | $^{184}\text{Re}$ , $^{188}\text{Re}$ |

## REFERENCES

- Manual for Reactor Produced Radioisotopes // IAEA-TECDOC-1340. 2003.
- S. Sudar, F. Cserpak, S.M. Qaim. Measurements and Nuclear Model Calculations of Proton-Induced Reactions on  $^{103}\text{Rh}$  up to 40 MeV: Evolution of the Excitation Function of the Therapeutic Radionuclide  $^{103}\text{Pd}$  // *Appl. Rad. Isot.* 2002, v. 56, p. 821-831.
- W.K. Roberts, U.O. Häfeli. Modeling rhenium-186 and rhenium-188 distribution in a neutron-activated rhenium wire and effect of the distribution on beta dosimetry in a water phantom // *Appl. Rad. Isot.* 1999, v. 51, p. 541-549.
- E. Persico, M.L. Bonardi, F. Groppi, et al. Excitation-functions and yields for Re-186g production by proton cyclotron irradiation // *Proc. of 18 Int. Conf. "Cyclotrons and their Applications"*. 2007, p. 248-250.

5. *Making Medical Isotopes:* Report on the Task Force on Alternatives for Medical Isotopes Production. TRIUMF, Canada, 2008. www.triumf.ca/ report-medical-isotope-production.
6. T.V. Malykhina et al. Investigation of the mixed X,n-radiation field at photonuclear production of isotopes // *PAST. Series "NPI"*. 2008, №5(50), p. 184-188.
7. V.L. Uvarov et al. Two-channel Mode of Mo-99 Production at an Electron Accelerator // *Proc. Conf. IPAC 2011, San Sebastian, Spain*. 2011, p. 3627-3629.
8. V.I. Nikiforov et al. A system for measuring the flux profile of high-energy bremsstrahlung // *PAST. Series "NPI"*. 2008, №3(49), p. 196-200.
9. N.I. Aizatsky, V.I. Beloglazov, V.P. Bozhko, et al. Nuclear-physical complex based on a 100 MeV electron linear accelerator // *PAST. Series "NPI"*. 2010, № 2(53), p. 18-22.
10. F. Salvat, J.M. Fernández-Varea, J. Sempau. PENELOPE-2008 a Code System for Monte-Carlo Simulation of Electron and Photon Transport // *OECD NEA (Issy-les-Moulineaux) France*. 2008.
11. V.I. Nikiforov and V.L. Uvarov. Development of the Technique Embedded into a Monte Carlo Transport System for Calculation of Photonuclear Isotope Yield // *Nukleonika*. 2012, v. 57(1), p. 75-80 (in Russian).
12. Handbook on photonuclear data for Applications // *IAEA. TECDOC-1178*. 2000.
13. N.I. Aizatsky et al. A powerful electron linear accelerator with energy up to 40 MeV // *PAST. Series "NPI"*. 2008, № 3(49), p. 25-29.

*Article received 23.10.2013*

### **ПОЛУЧЕНИЕ ИЗОТОПОВ Pd И Re В ПОЛЕ СМЕШАННОГО X,n-ИЗЛУЧЕНИЯ УСКОРИТЕЛЯ ЭЛЕКТРОНОВ**

***Н.П. Дикий, В.А. Кушнир, Ю.В. Ляшко, В.В. Митроченко, С.А. Пережогин, Ю.В. Рогов, А.Э. Тенишев, А.В. Торговкин, В.Л. Уваров, В.А. Шевченко, И.Н. Шляхов, Б.И. Шраменко***

Радиоактивные изотопы палладия ( $^{103}\text{Pd}$ ) и рения ( $^{186}\text{Re}$  и  $^{188}\text{Re}$ ) широко используются в ядерной медицине. Изучаются условия их получения фотоядерным методом на ускорителе электронов. Исследованы каналы наработки целевых изотопов и примесей при облучении мишеней из палладия и рения природного изотопного состава смешанным потоком тормозного излучения с граничной энергией 40 МэВ и фотонейтронов. Путем размещения конвертера тормозного излучения и мишени внутри модератора нейтронов получены данные по влиянию спектра фотонейтронов на выход изотопов. Методом моделирования изучена также зависимость фотоядерного выхода целевых изотопов и основных примесей от энергии электронов.

### **ОТРИМАННЯ ІЗОТОПІВ Pd І Re В ПОЛІ ЗМІШАНОГО X,n-ВИПРОМІНЮВАННЯ ПРИСКОРЮВАЧА ЕЛЕКТРОНІВ**

***М.П. Дикий, В.А. Кушнір, Ю.В. Ляшко, В.В. Митроченко, С.О. Пережогін, Ю.В. Рогов, А.Е. Тенишев, О.В. Торговкін, В.Л. Уваров, В.А. Шевченко, І.М. Шляхов, Б.І. Шраменко***

Радіоактивні ізопадію ( $^{103}\text{Pd}$ ) та ренію ( $^{186}\text{Re}$  і  $^{188}\text{Re}$ ) широко використовуються в ядерній медицині. Вивчаються умови їх отримання фотоядерним методом на прискорювачі електронів. Досліджено канали напрацювання цільових ізопадію і домішок при опромінуванні мишеней з паладію і ренію природного ізопадію складу змішаним потоком гальмівного випромінювання з граничною енергією 40 МеВ і фотонейтронів. Шляхом розміщення конвертера гальмівного випромінювання і мишені усередині модератора нейтронів отримано дані щодо впливу спектра фотонейтронів на вихід ізопадію. Методом моделювання вивчена також залежність фотоядерного виходу цільових ізопадію і основних домішок від енергії електронів.